

Finite-width effects in the near-threshold ZZZ and ZW^+W^- production at ILC

R. S. Pasechnik¹ and V. I. Kuksa²

¹*Uppsala University, Box 516, SE-751 20 Uppsala, Sweden and*

²*Institute of Physics, Southern Federal University, 344090 Rostov-on-Don, Russia*

We calculate the cross-section of the near-threshold off-shell ZZZ and ZW^+W^- production at the International Linear Collider taking into account their instability and the principal part of NLO corrections. The calculations are performed in the framework of the model of unstable particles with smeared mass-shell. We show that the contribution of the finite Z/W and H widths (their instability) is large in the Higgs resonance range and should be taken into account in the Higgs boson searches at future colliders.

A great amount of work has been done so far in precision tests of the Standard model (SM) including measurements of gauge boson, top quark masses and widths at LEP II [1, 2] and Tevatron [3], and very recently at much higher energies at LHC (see e.g. Ref. [4]). Due to clean environment and energies well above the electroweak (EW) scale, future linear colliders would provide important tools for high-precision investigation of gauge bosons and Higgs physics in the SM and beyond [5, 6].

The multiple production of the gauge bosons is crucial for probing gauge boson (and Higgs) self-couplings, and thus for testing the non-Abelian structure and EW symmetry breaking of the SM. The processes of two- (ZZ and W^+W^-) and three-boson (ZZZ and ZW^+W^-) production are of major importance as they give a direct information on trilinear and quartic vector boson couplings.

Triple couplings of the neutral (Z and γ) and charged (W^\pm) EW bosons, which were measured at LEP II [7, 8] and Tevatron [9], demonstrated a good agreement with the SM prediction within a few percent [1]. For this purpose, the NLO EW *factorizable* corrections and *finite-width effects* (FWE) in the off-shell boson pair production i.e. $e^+e^- \rightarrow V^*V^* \rightarrow 4f$ are very important, especially, in the near-threshold energy region (see e.g. Refs. [10, 11]). However, corresponding higher-order calculations in the framework of traditional perturbation theory (PT) are rather cumbersome for $2 \rightarrow 4$ processes as require evaluation of a few thousands one-loop diagrams, and various schemes for automated loop calculations are practically applied [12, 13].

Triple massive gauge boson (ZZZ and ZW^+W^-) production processes can be utilized to probe quartic gauge couplings and anomalous couplings in the Higgsstrahlung process (see, e.g. Ref. [14–16]). At the moment, these processes being intensively studied in literature [17–20]. Typical leading-order contributions are shown in Fig. 1. In this work, we are primarily concentrated on the three-boson production processes in the Standard Model at ILC as the simplest case.

Generally, FWE in a multiple gauge bosons production are closely connected to their instability, so they are usually referred to as the unstable particles (UP).

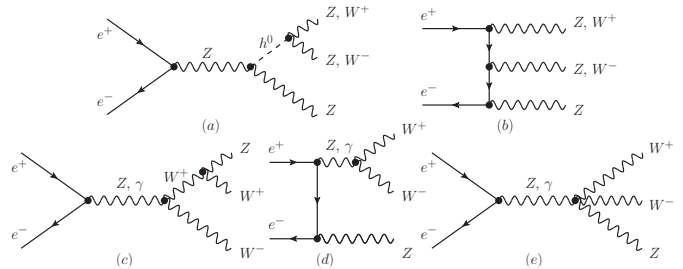


FIG. 1: Diagrams for $e^+e^- \rightarrow ZZZ, ZW^+W^-$ processes.

Near-threshold production of the unstable particles, as a rule, is accompanied by large FWE, which must be taken into account in analysis of corresponding observables [10, 11]. In addition to the standard PT approach to FWE analysis, based on the stable particles approximation (SPA), where UP instability is accounted for by higher-order corrections, various approximation schemes are practically applied in the literature, namely, semi-analytical approximation [21, 22], improved Born approximation [23], asymptotical expansions of the cross section in powers of coupling constant [24], fermion loop scheme, etc (see, also Ref. [25, 26] and references therein). All above mentioned methods are based on the traditional quantum field theory of unstable particles [21]. At the same time, there are some alternative approaches for UP description such as the effective theory of UP [27], modified perturbation theory [28] and the smeared-mass unstable particles model [29, 30].

The main feature of the FWE is the “smearing” (fuzzing) of the threshold. In the standard treatment, this effect is described by taking into account all virtual states of UP, i.e. by its off-shellness. So, the cross section $\sigma(e^+e^- \rightarrow VV)$ is defined as the cross section of inclusive four-fermion production $\sigma(e^+e^- \rightarrow 4f)$ in the double-pole approximation [31], which selects only diagrams with two nearly resonant V bosons and the number of contributing graphs is considerably reduced. Such an approximate description is usually realized with the help of the dressed UP propagators.

In order to describe FWE in triple boson produc-

tion we have to consider full cascade process $e^+e^- \rightarrow ZZZ, ZW^+W^- \rightarrow \sum_f 6f$, where the instability of the off-shell bosons is described by Breit-Wigner propagators. So far, full NLO calculations were performed in the case of on-shell bosons only in the stable-particle approximation, i.e. without taking into account FWE and only for light SM Higgs boson with masses $M_H = 120\text{ GeV}$ and 150 GeV [18–20]. The corresponding calculations in the traditional perturbation theory are rather cumbersome, as requires the complete set of a few thousands of one-loop diagrams.

In the off-shell case, one encounters a very complicated problem. Exact NLO $2 \rightarrow 6$ matrix elements would require analytical evaluation of many tens of thousands loop diagrams, and are not available at the moment, but they are very important for boson FWE and Higgs contribution studies in vicinity of the threshold and Higgs resonance with the biggest cross section.

In this paper, we describe FWEs in the near-threshold triple boson production $e^+e^- \rightarrow Z^*Z^*Z^*, Z^*W^{+*}W^{-*} \rightarrow \sum_f 6f$ within the framework of the smeared-mass unstable particles (SMUP) model developed in Ref. [29, 30]. In Ref. [32] the conception of the mass smearing as the main element of the SMUP model was successfully tested by comparison of its predictions with LEP II data on the boson-pair production $e^+e^- \rightarrow Z^*Z^*, W^{+*}W^{-*} \rightarrow \sum_f 4f$ total cross sections and Monte-Carlo simulations including full next-to-leading order matrix elements. In the framework of this model, the off-shell vector bosons Z, W^\pm are treated as unstable particles, and the smearing of their mass shell effectively accounts for all-order propagator type corrections; the principal part of other factorisable corrections can effectively be taken into account as suggested in Ref. [32].

In this work, we present the total (inclusive) cross-sections of the off-shell ZZZ, ZW^+W^- bosons production including FWE and the principal part of NLO (factorizable) corrections coming from the initial state radiation (ISR) and fussy-mass-shell unstable vector bosons in the framework of SMUP model. We found a large finite-width effect for Higgs masses $M_H \gtrsim 2M_W, 2M_Z$, when the contribution of Higgs diagrams becomes dominant and very sensitive to the Higgs boson width. So, this effect should be taken into consideration and can be applied as an auxiliary tool in Higgs boson searches at future colliders.

BASICS OF THE SMUP MODEL

In the off-shell ZZZ and ZW^+W^- boson production in order to take into account FWE in standard way we need to consider full cascade process with six-particle final state and intermediate-state unstable Z and W bosons (see Fig. 2).

There is another way to tackle the issue. The SMUP model [29, 30] provides the possibility to treat Z and W bosons as final state particles and simultaneously to take into account their instability and obtain the finite-width effects correctly by smearing their mass shells [32, 33]. In this Section, we give a short description of the principal elements of the SMUP model and its advantages compared to the standard treatment (for more detail review of the SMUP model, see Ref. [30, 33] and references therein).

The UP wave function in the framework of SMUP model is given by

$$\Phi_a(x) = \int \Phi_a(x, \mu) \omega(\mu) d\mu, \quad (1)$$

where $\Phi_a(x, \mu)$ is the standard spectral component which defines a particle with a fixed mass squared $m^2 = \mu$ in the stable (fixed-mass) particle approximation (SPA). The weight function $\omega(\mu)$ is then accounts for the self-energy interactions of the UP with vacuum fluctuations and decay products. This function includes all the information about UP decay properties (its instability) and describes the smeared (“fuzzed”) mass-shell of the UP. The “fuzzing” of the UP mass shell is then caused, on the one hand, by quantum-mechanical instability according to the time-energy uncertainty relation and, on the other hand, by stochastic interactions of the UP with the electro-weak vacuum fluctuations.

Then, the (anti)commutative relations for the UP field operators have an additional δ -function in the “smeared” UP mass [30]

$$[\Phi_\alpha^-(\bar{k}, \mu), \Phi_\beta^+(\bar{q}, \mu')]_\pm = \delta(\mu - \mu') \delta(\bar{k} - \bar{q}) \delta_{\alpha\beta}, \quad (2)$$

Here, subscripts “ \pm ” correspond to the fermion and boson fields. The presence of $\delta(\mu - \mu')$ in Eq. (2) means that the acts of creation and annihilation of the unstable particles with different μ do not interfere. So the quantity μ has the status of the physically distinguishable value of the UP mass squared m^2 .

In the model under consideration, the transition amplitude of the UP decay $\Phi \rightarrow \phi_1 \phi_2$ directly follows from Eqs. (1) and (2), and can be written as [30]

$$A(k, \mu) = \omega(\mu) A^{st}(k, \mu), \quad (3)$$

where $A^{st}(k, \mu)$ is the corresponding amplitude in the SPA, which is calculated in the standard way to a given order of the Perturbation Theory. From Eq. (3) it follows that the differential (in UP mass squared μ) probability of the transition is $dP(k, \mu) = \rho(\mu) |A(k, \mu)|^2 d\mu$, where $\rho(\mu) = |\omega(\mu)|^2$ is probability density of mass parameter $\mu = m^2$. This function is induced by multiple UP interactions with collective (in our case, EW) vacuum fluctuations of self-energy type and with decay products (vertex-type corrections). In general, it is of non-perturbative nature and can be modeled in various ways. In this work,

we use the Lorentz distribution function [30]

$$\rho(\mu) = \frac{1}{\pi} \frac{\text{Im} \Pi(\mu)}{[\mu - m^2(\mu)]^2 + [\text{Im} \Pi(\mu)]^2}, \quad (4)$$

where $\Pi(k^2)$ is the conventional vacuum polarisation function, $m^2(\mu) = m_0^2 + \text{Re} \Pi(\mu)$ with bare UP mass m_0 . The distribution (4) is of the Breit-Wigner type and accounts for the electro-weak quantum fluctuations of UP mass shell analogous to ones leading to a dressing up of the full propagator of an off-shell particle in the conventional quantum field theory. It naturally appears in the effective theory of UP as the most suitable one in the high-energy processes [30], and was tested before against LEP II data on off-shell ZZ and W^+W^- near-threshold production [32].

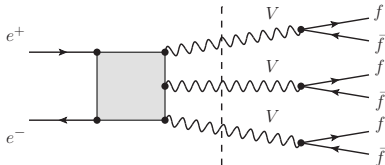


FIG. 2: Schematic illustration of the exact factorization of the total $ee \rightarrow VVV \rightarrow 6f$ cross-section in the SMUP model.

As a general feature, such a model allows to consider the UP as the final state particles and their instability is then included by a convolution of decay widths or cross sections with UP mass probability density $\rho(m_i^2)$ in each UP leg due to exact factorisation property which was proven previously in Ref. [34]. As a consequence of UP mass-smearing effect, this factorisation drastically simplifies the calculations. Now, we wish to apply the formalism of SMUP model for prediction of the finite-width effects in the triple off-shell (ZZZ and ZW^+W^-) bosons production.

MASS-SHELL SMEARING EFFECTS IN THE TRIPLE BOSONS PRODUCTION

The processes $e^+e^- \rightarrow ZZZ; ZW^+W^-$ at the tree level (leading order) in SPA are described by the set of diagrams represented in Fig. 1. Here, ZZZ production is described by nine diagrams with topologies a, b , whereas ZW^+W^- production is given by sixteen diagrams a, \dots, e . The first subset of diagrams a has a resonant character at $M_H \gtrsim 2M_W, 2M_Z$, and plays significant role in the Higgs and FWE contributions. Complete NLO corrections to on-shell bosons production are described by additional few thousands diagrams, which were calculated in Refs. [18–20].

Due to exact factorisation property, the SMUP model [30, 34] allows to represent the total cross-section of the inclusive process $e^+e^- \rightarrow ZZZ, ZW^+W^- \rightarrow \sum_f 6f$ in

the factorized triple-convolution form (as schematically illustrated in Fig. 2)

$$\sigma(s) = \int \int \int dm_1^2 dm_2^2 dm_3^2 \sigma(s; m_1^2, m_2^2, m_3^2) \times \rho(m_1^2) \rho(m_2^2) \rho(m_3^2), \quad (5)$$

where $\sigma(s; m_1^2, m_2^2, m_3^2)$ is the Born-level cross-section as a function of different bosons masses squared m_i^2 , $i = 1, 2, 3$ in the SPA, $\rho(m_i^2)$ is the probability distribution of the boson mass squared in i th leg given by Eq. 4. The Born ZZZ and ZW^+W^- production cross-sections were calculated using FeynCalc v6.1 [13] as functions of smeared masses of Z and W^\pm bosons m_i^2 , and then their convolutions with $\rho(m_i^2)$ over variable m_i^2 are performed numerically. In order to treat the poles in the boson propagators, which arise in the Higgs resonance region in the integration over the phase space of the boson pairs, we introduce the q^2 -dependent decay width of Higgs boson in the propagator [35]

$$\Gamma_H(q) = \Gamma_H^{st}(q) + \Gamma_H^{WW}(q) + \Gamma_H^{ZZ}(q), \quad (6)$$

where $\Gamma_H^{st}(q)$ is standard width of Higgs at the pole $M_H^2 = q^2$ [32] and other two terms account for the boson-pair channels of the Higgs decay. It should be noted here, that the exact Higgs width as a function of the momentum transfer scale (6) is very important since it determines to a large extent the ZZZ and ZW^+W^- production cross sections in the resonance regions, giving rise to the possibility of probing Higgs decay properties. If Higgs boson is heavier than 160 GeV and behaves as predicted by the Standard Model, it decays predominantly into gauge-boson pairs and subsequently into four light fermions. And triple boson production at ILC can be rather sensitive to extra (anomalous) contributions to the HVV coupling from the new physics [16].

The approach under discussion has a close analogy with the convolution method [36] and the semi-analytical approximation [21, 22]. However, the status of these approaches are different [30, 32, 33]. In the framework of the SMUP model, the expression (5) directly follows from the UP smearing-mass conception, and the function $\rho(m_i^2)$ describes the probability distribution in UP mass squared [29, 30]. Moreover, the definition of the unstable particle field function (1) determines the strategy of taking into account the major part of the higher-order corrections in the near-threshold energy domain [32, 33].

CROSS SECTIONS OF ZZZ AND ZW^+W^- PRODUCTION AT ILC

In the framework of SMUP model, the FWE were previously studied in the boson-pair production $e^+e^- \rightarrow ZZ, W^+W^-, ZH, Z\gamma$ at LEP II in Refs. [32, 33]. In the boson-pair production in vicinity of the threshold, the

NLO EW corrections are dominated by factorizable corrections to EW couplings, propagator-type (self-energy) corrections and the soft/hard initial and final state radiation while boxes, pentagons, etc can become relevant only at energies far from the threshold ones [26].

As the next natural step, we apply the same strategy in analysis of the triple boson production. For this purpose, we perform the following consistency check – we compared our $e^+e^- \rightarrow ZZZ$ and ZW^+W^- production cross sections in the SPA including only initial state radiation and NLO vertex corrections (renormalisation of the boson couplings) with full NLO results from Refs. [19, 20] in the 50 GeV range nearby to the threshold and got very close results within a percentage accuracy. This basically proves that non-factorisable, box and pentagon diagrams do not significantly contribute to the near-threshold production cross section, and can be omitted for our purposes. This is the only approximation we adopt in our calculations.

Then we recalculated the on-shell ZZZ and ZW^+W^- production cross-sections at fixed $M_H = 120$ GeV in SPA taking into account Higgs boson FWE. Again, the results coincide with ones reported in Ref. [19, 20]. The contribution of Higgs diagrams and gauge boson FWE into the total cross-section at $M_H = 120$ GeV turns out to be relatively small. It is therefore very instructive to look at these contributions for heavier Higgs boson.

The cross-section of the process $e^+e^- \rightarrow ZW^+W^-$ as function of \sqrt{s} at fixed $M_H = 175$ GeV (just above the latest Tevatron exclusion limit [37]) is shown in Fig. 3. The Born cross sections in SPA and with taking into account the Z/W FWE (due to the instability of gauge bosons in the final state) in the framework of SMUP model are represented by solid and dashed lines, respectively. The corresponding cross-section including the initial state radiation (ISR) corrections is given by the dashed-dotted line. These corrections together with the UP propagator-type corrections effectively taken into account by UP mass-smearing effects in the framework of SMUP model are the main part of NLO corrections at considered energies [32]¹. One can see from Fig. 3 that the contribution of Z/W FWE is occurred to be quite large for relatively heavy Higgs boson in the near-threshold region.

In Fig. 4, the Born cross-section is shown as function of Higgs mass M_H at various fixed energies. Solid lines represent the total cross-section while the dashed lines – the part given by Higgs-less diagrams only. This figure illustrates rather strong dominance of the Higgs contribu-

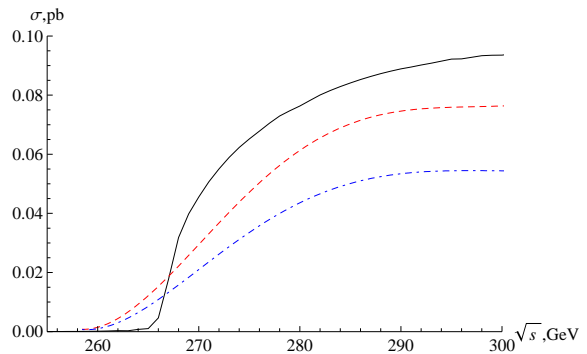


FIG. 3: Cross-section of the process $e^+e^- \rightarrow ZW^+W^-$ at fixed Higgs mass $M_H = 175$ GeV, given at leading order in SPA (solid line), including gauge bosons FWE (dashed line) and with taking into account both FWE and ISR corrections (dash-dotted line).

tion due to Higgs resonance in the W^+W^- phase space. It is worth to note here that the gauge boson FWE and smearing-mass effects naturally decrease at larger energies, and get practically negligible at $\sqrt{s} \gtrsim 450$ GeV.

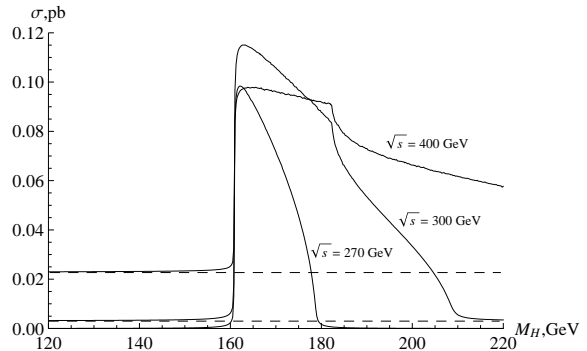


FIG. 4: Cross-section of the process $e^+e^- \rightarrow ZW^+W^-$ as function of M_H at different energies. Contributions of the Higgs-less diagrams only are given by dashed lines.

Analogously, the cross-section of the process $e^+e^- \rightarrow ZZZ$ as function of \sqrt{s} at fixed $M_H = 195$ GeV close to the $H \rightarrow ZZ$ threshold is given by Fig. 5, with the same notations as before. In Fig. 6, the Born cross-section is shown as function of Higgs mass at different fixed energies. Again, similarly to the ZW^+W^- case, the contributions of gauge bosons and Higgs FWE is large in the near-threshold region close to the Higgs resonance.

In Conclusion, we would like to notice that using the argument that the mass-smearing conception realized in the smeared-mass unstable particles model is in the good agreement with the LEP II experimental data on the near-threshold boson-pair production, we applied the same ideas to off-shell ZZZ and ZW^+W^- boson production at linear collides. The approach under consideration significantly simplifies the calculations with respect to

¹ The major part of the vertex EW corrections at the threshold can be effectively included by taking coupling constants at the M_Z mass scale, while contribution from the renormalisation group evolution is small at energies close to the threshold [32].

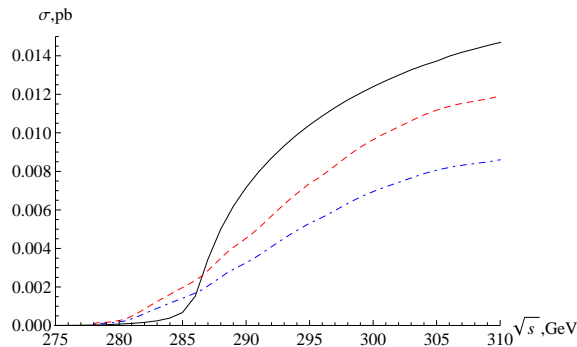


FIG. 5: Cross-section of the process $e^+e^- \rightarrow ZZZ$ at fixed Higgs mass $M_H = 195$ GeV. Notations here are the same as in Fig. 3.

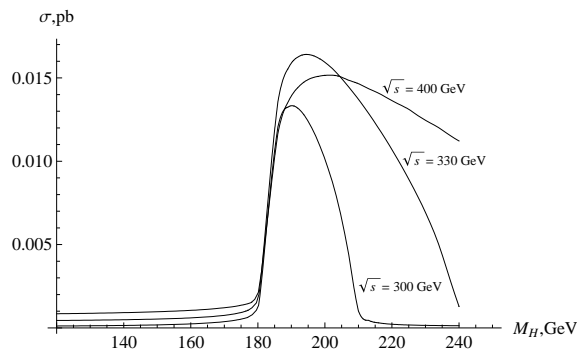


FIG. 6: Cross-section of the process $e^+e^- \rightarrow ZZZ$ as function of M_H at different energies.

the traditional one due to the exact factorization property. Explicit calculations of the triple-boson production cross sections demonstrate rather strong dependence of the gauge boson finite-width effects on the Higgs boson mass. In the near-threshold energy domain such effects are large and comparable with the initial state radiation corrections when the Higgs-resonant contribution is significant, and small when the Higgs contribution is negligible. The Higgs-resonant contribution into the total cross-section is strongly dominant and have well-defined signature at Higgs masses above the Higgs decay threshold $M_H \gtrsim 2M_W$ for ZW^+W^- production and at $M_H \gtrsim 2M_Z$ for ZZZ production.

Useful discussions with Rikard Enberg, Gunnar Ingelman, Oscar Stål and Glenn Wouda are gratefully acknowledged. This work was partially supported by the Carl Trygger Foundation.

[1] J. Alcaraz *et al.*, arXiv:0712.0929.
[2] R. Barate *et al.*, Phys. Lett. **B565**, 61-75 (2003).
[3] J. Zhu, AIP Conf. Proc. **1182**, 152-155 (2009).
[4] The ATLAS Collaboration, CERN-PH-EP-2010-037, arXiv:1010.2130.

[5] G. Aarons *et al.*, arXiv:0709.1893.
[6] The ILD Concept Group, DESY-2009-87, FERMILAB-PUB-09-682-E, KEK-REPORT-2009-6, arXiv:1006.3396.
[7] G. Abbiendi *et al.*, Eur. Phys. J. **C19**, 1-14 (2001).
[8] J. Abdallah *et al.*, Eur. Phys. J. **C51**, 525-542 (2007).
[9] V. M. Abazov *et al.*, Phys. Rev. Lett. **100**, 131801 (2008).
[10] T. Muta, R. Najima, S. Wakaizumi, Mod. Phys. Lett. **A1**, 203 (1986).
[11] A. Denner, T. Sack, Z. Phys. **C45**, 439 (1990).
[12] A. Denner, Fortsch. Phys. **41**, 307-420 (1993).
[13] T. Hahn, M. Perez-Victoria, Comput. Phys. Commun. **118**, 153-165 (1999); T. Hahn, Comput. Phys. Commun. **140**, 418-431 (2001); PoS **ACAT08**, 121 (2008).
[14] G. Belanger, F. Boudjema, Phys. Lett. **B288**, 210-220 (1992); Phys. Lett. **B288**, 201-209 (1992).
[15] C. Grosse-Knetter, D. Schildknecht, Phys. Lett. **B302**, 309-378 (1993).
[16] W. Kilian, M. Kramer, P. M. Zerwas, Phys. Lett. **B381**, 243-247 (1996); S. S. Biswal, R. M. Godbole, R. K. Singh *et al.*, Phys. Rev. **D73**, 035001 (2006).
[17] V. D. Barger, T. Han, R. J. N. Phillips, Phys. Rev. **D39**, 146 (1989).
[18] S. Ji-Juan, M. Wen-Gan, Z. Ren-You *et al.*, Phys. Rev. **D78**, 016007 (2008).
[19] S. Wei, M. Wen-Gan, Z. Ren-You *et al.*, Phys. Lett. **B680**, 321-327 (2009).
[20] F. Boudjema, L. D. Ninh, S. Hao *et al.*, Phys. Rev. **D81**, 073007 (2010).
[21] D. Bardin and G. Passarino, *The Standard Model in the Making* (Oxford University Press, 1999).
[22] D. Y. Bardin, M. S. Bilenky, D. Lehner *et al.*, Nucl. Phys. Proc. Suppl. **37B**, 148-157 (1994); D. Y. Bardin, D. Lehner, T. Riemann *et al.*, hep-ph/9602339.
[23] S. Dittmaier *et al.*, Nucl. Phys. B **376**, 29 (1992).
[24] M. L. Nekrasov, 0709.3046.
[25] A. Denner *et al.*, Phys. Lett. B **612**, 223 (2005); Nucl. Phys. B **724**, 247 (2005).
[26] W. Beenakker *et al.*, in *Physics at LEP2*, eds. G. Altarelli, T. Sjöstrand and F. Zwirner (CERN 96-01, Geneva, 1996), Vol. 1, p. 79; arXiv:hep-ph/9602351.
[27] M. Beneke, A. P. Chapovsky, A. Signer *et al.*, Phys. Rev. Lett. **93**, 011602 (2004).
[28] M. L. Nekrasov, hep-ph/0002164.
[29] P. T. Matthews and A. Salam, Phys. Rev. **112**, 283 (1958).
[30] V. I. Kuksa, Phys. Lett. **B633**, 545-549 (2006); Int. J. Mod. Phys. **A24**, 1185-1205 (2009).
[31] A. Denner *et al.*, Nucl. Phys. B **440**, 95 (1995); Nucl. Phys. B **519**, 39 (1998); W. Beenakker *et al.*, Nucl. Phys. B **548**, 3 (1999).
[32] V. I. Kuksa and R. S. Pasechnik, Int. J. Mod. Phys. A **24**, 5765 (2009); Int. J. Mod. Phys. A **23**, 4125 (2008).
[33] V. I. Kuksa and R. S. Pasechnik, Phys. Atom. Nucl. **73**, 1622 (2010);
[34] V. I. Kuksa, N. I. Volchanskiy, Int. J. Mod. Phys. **A25**, 2049-2062 (2010); V. I. Kuksa, Phys. Atom. Nucl. **72**, 1063-1073 (2009).
[35] A. Bredenstein, A. Denner, S. Dittmaier *et al.*, Phys. Rev. **D74**, 013004 (2006).
[36] G. Altarelli, L. Conti, V. Lubicz, Phys. Lett. **B502**, 125-132 (2001).
[37] B. Kilminster, talk at International Conference for High Energy Physics (ICHEP 2010), Paris, France July 22 - 28 2010.